Agricultural Systems 164 (2018) 58–70

Contents lists available at ScienceDirect

Agricultural Systems

journal homepage: www.elsevier.com/locate/agsy

Predicting local-scale impact of climate change on rice yield and soil organic carbon sequestration: A case study in Roi Et Province, Northeast Thailand

Noppol Arunrat[a,*], Nathsuda Pumijumnong[a], Ryusuke Hatano[b]

[a] Faculty of Environment and Resource Studies, Mahidol University, Salaya, Phutthamonthon, Nakhon Pathom 73170, Thailand
[b] Laboratory of Soil Science, Graduate School of Agriculture, Hokkaido University, Kita 9 Nishi 9, Kita-ku, Sapporo 060-8589, Japan

ARTICLE INFO

Keywords:
Climate change
EPIC model
Rice
Soil organic carbon
Thailand

ABSTRACT

Climate change poses a serious threat to rice production and soil quality in tropical monsoon areas where it is the lifeline of regional food security. In this study, the Environmental Policy Integrated Climate (EPIC) model was evaluated for the reliability of model calibration and validation procedures using local-scale data. The model was then employed to evaluate the possible impact of climate change on rice yield and soil organic carbon (SOC) sequestration in Roi Et Province, Northeast Thailand. The dominant factors that influence the changes in rice yield and SOC sequestration were identified. Four Representative Concentration Pathway (RCP) scenarios (RCPs 2.6, 4.5, 6.0, and 8.5) and Sixteen General Circulation Models under four future time periods; near future (2020–2039), mid future (2040–2059), far future (2060–2079), and very far future (2080–2099) from the Coupled Model Intercomparison Project Phase 5 (CMIP5) were used as future climate projections. The findings revealed that climate change will impact rice yields positively, which will benefit farmers, especially in rain-fed areas, by +2.6% (RCP8.5: 2080–2099) to +22.7% (RCP6.0: 2080–2099). Rice yields in all case tend to increase significantly by +0.7% (RCP8.5: 2060–2079) to +18.8% (RCP6.0: 2080–2099), with the exception of 2080–2099 under RCP8.5, which results in a decline of rice yield by −8.4%. The precipitation is the most important factor for rice yield in this area. Although rising temperatures will bring a slight rice yield reduction, its impact will be negated by large amounts of increased CO_2 concentration and precipitation. Conversely, SOC decreased significantly in all time periods. The highest decreased SOC was a -32.0% decline under RCP8.5 in the very far future. This is because rises in temperature and precipitation, with precipitation being the most important driver, negated the enrichment of CO_2 fertilization, resulting in accelerated SOC decomposition rates, which may increase nitrogen availability to the soil and increase yield.

1. Introduction

According to the Fifth Assessment Report of the Intergovernmental Panel on Climate Change (IPCC, 2013 AR5), the global mean temperature has risen by about 0.85 °C during the period of 1880 to 2012. It also states that the global mean surface temperature will increase by 0.3 to 4.8 °C by the end of 21st century (IPCC, 2013). Thus, climate change and rising atmospheric CO_2 concentrations may influence rice yields (Parry et al., 2004; Adejuwon, 2005) and thus threaten food security (Nguyen, 2006). In the tropics, crop production is more sensitive to warming since they already operate close to the optimal temperature, hence, the yield may reduce sharply (Oteng-Darko et al., 2012; Candradijaya et al., 2014). The climate of Thailand is experiencing a gradual warming, as indicated by significant changes of temperature and rainfall extreme trends from observed records (Limjirakan and Limsakul, 2012; Limsakul et al., 2010). Increased dry season rainfall in Northeast Thailand was found to be consistent with wider ongoing climate dynamics observed in East Asia and explained by the weakening of the East Asian winter monsoon (Zhou, 2011). These changes were attributed to global warming (Zhang et al., 2011), indicating that temperature is likely to continue increasing in the future. Although soils have the potential to mitigate increasing CO_2 concentrations through carbon (C) sequestration, land misuse and soil mismanagement have caused the depletion of soil organic carbon (SOC) (Li and Zhang, 2007; Li et al., 2010). Therefore, computer simulation models of soil, crop yields, and atmospheric systems can make valuable contributions to determining crop responses, predicting crop performances, and evaluating the environmental impacts of different management practices.

The Environmental Policy Integrated Climate (EPIC) model, a

* Corresponding author.
E-mail address: noppol.aru@mahidol.ac.th (N. Arunrat).

https://doi.org/10.1016/j.agsy.2018.04.001
Received 3 May 2017; Received in revised form 27 March 2018; Accepted 3 April 2018
Available online 16 April 2018
0308-521X/ © 2018 Elsevier Ltd. All rights reserved.

notable integrated model of management of the soil–water–atmosphere system, was developed and has been successfully used to simulate the effects of this system on crop production and soil dynamics (Williams et al., 1984; Williams et al., 1989; Sharpley and Wiliams, 1990); Williams et al. (2006) noted that the EPIC model can also be used to simulate nitrogen (N) and C cycling, surface runoff and leaching of N and phosphorous (P), alternative cropping systems, management practices, crop growth and yields of about 100 different crop plant species, climate change, and the effects of atmospheric CO_2 concentration. According to Zhao et al. (2013), the EPIC model is the most suitable model for SOC simulation for different irrigation, fertilization, and tillage treatments. With increasing concern about climate change and associated issues, the EPIC model has increasingly been used to simulate the impacts of climate change on crop yields (Brown et al., 2000; Izaurralde et al., 2003; Wang and Li, 2010), SOC (Causarano et al., 2007, 2008; Gaiser et al., 2008; Zhang et al., 2010; Balkovic et al., 2011), and nitrate leaching (Chung et al., 2001). However, these studies have been conducted at large scales (basin, country, or regional), at which local heterogeneity in factors such as local climate, soil properties, and farmer management practices could not be incorporated. The impacts of climate change at different scales may differ in severity.

Indeed, local-scale simulation is often challenging because precise data are rarely available and accessible. For instance, Xiong et al. (2008) examined the performance of CERES-Rice at a regional scale across China using a cross-calibration process based on limited experimental data, agroecological zones, and a geographical database with a 50 km × 50 km grid scale; reducing the error between the simulated and actual yields using specific areas and other yield loss factors was suggested. Niu et al. (2009) reported that the use of field measurement data or location-specific data instead of data from widely available sources decreased the simulation bias in a study in which the EPIC model was used to simulate grain sorghum yields in the US Great Plains under different climate scenarios. Causarano et al. (2011) suggested that more data on spatial and temporal variation in SOC are needed to improve the calibration and validation of the EPIC model. Xiong et al. (2014) suggested that more precise data at the local or regional scale could improve the reliability and accuracy of model calibration even for global simulation of rice yields with the EPIC model. However, to the best of our knowledge, no study has assessed the potential impacts of climate change on rice yield and SOC dynamics in Roi Et province, in the northeast region of Thailand (although see Arunrat, 2017). The work by Arunrat (2017) used EPIC0509 model and A2 and B2 scenarios to predict rice yield and SOC in Roi Et province, but the climate scenarios and model version were out of date and it is still unclear what is the most dominant climate factor controlling rice yield and SOC changes. Tao et al. (2006 and 2014) suggested that the effects of temperature and CO_2 concentration on physiological processes and mechanisms for crop growth and production should be separately investigated. Also, Hobley and Wilson (2016) proposed that precipitation and temperature control soil C dynamics at the regional scale. Therefore, it is clear that using further new climate scenarios and model versions are needed to bring robust predictions of climate change impact to future rice yield and SOC in this area.

To fill a remaining gap in this research, there is a pressing need to improve the accuracy of model simulations through the use of location-specific data for model calibration and validation. In the present study, the EPIC0810 version was used and run using the i-EPIC (interactive EPIC) interface. The objectives of this study are: 1) to evaluate the reliability of the EPIC model calibration and validation processes based on local-scale data, 2) to evaluate the possible impacts of climate change on rice yield and SOC sequestration, and 3) identify the most important factors that influence the changing of rice yields and SOC sequestration in this area.

2. Materials and methods

2.1. Site description

The study area is in the Thung Kula Sub-district, Suwannaphum District, Roi Et Province, Thailand, located at 15°28′N, 103°48′E. Roi Et soils are derived from washed deposits of sandstone and occur on the lower parts of peneplains. The elevation ranges from 100 to 200 m above sea level. This area has a tropical monsoon climate (Köppen "Aw"). The average annual precipitation in 2014 ranged from 800 to 2900 mm, and the mean annual air temperature ranged from 26 to 28 °C. The major soil type in Roi Et Province is ultisol with > 60% sand content; low SOC, ranging from 0.40%–1.29%; and moderately acidic surface soil with a pH range of 5.0–6.0 (LDD, 1991).

2.2. EPIC model description

2.2.1. Crop growth model

The EPIC model is able to simulate the growth of both annual and perennial crops based on a single crop growth model. This model uses radiation-use efficiency to calculate the photosynthetic production of biomass. Interception of solar radiation is estimated as a function of leaf area index (LAI). LAI is simulated with equations determined based on heat units, the maximum LAI for the crop, genetic coefficients, and five environmental stresses (water; temperature; nutrients, N and P; and aeration). The stress factor values range from 0 to 1, and the phonological development of the crop is based on daily heat unit accumulation and a heat unit index value (HUI) computed from 0 at planting to 1 at maturity. Atmospheric CO_2 concentration also influences photosynthesis by increasing radiation-use efficiency. Therefore, crop yields are estimated by multiplying the above-ground biomass at maturity (determined based on the accumulation of heat units or a specified harvest date) by a harvest index (economic yield divided by above-ground biomass) specified for the particular crop (Easterling et al., 1998; Liu et al., 2014).

2.2.2. Carbon flows in the EPIC model

The EPIC model simulates dynamic C processes using C routines conceptually similar to those used in the Century model (Izaurralde et al., 2001, 2006). The Century model (Parton et al., 1987, 1994) was successfully used to simulate soil organic matter (SOM) across a variety of land use types and climates and is among the models that consistently produce low errors and show low overall bias (Kelly et al., 1997; Smith et al., 1997). The total C pool for soil C estimations consists of five compartments: structural litter, metabolic litter, microbial biomass, slow humus, and passive humus. Parton et al. (1987, 1993, 1994) and Izaurralde et al. (2006) described the original dynamic C processes in the Century model and the new C and N modules developed for the EPIC model. These new modules were built to connect simulation of soil C and N dynamics with crop management, tillage methods, and erosion processes. The surface microbial pool turnover rate is independent of soil texture, whereas soil texture influences the turnover of active SOM (higher rates for sandy soils). The model assumes a 60% loss of carbon due to microbial respiration for surface microbes and 55% for all other layers. Allocation of carbon from lignin in structural litter to CO_2 is set at 0.3, and the rest is partitioned into slow humus. In each process, there are moisture and temperature controls on soil biological processes (Izaurralde et al., 2006).

2.3. Data collection and model input data

2.3.1. Simulation unit

The study area was divided into small sub-areas to collect soil samples, prepare climate data, and determine land management

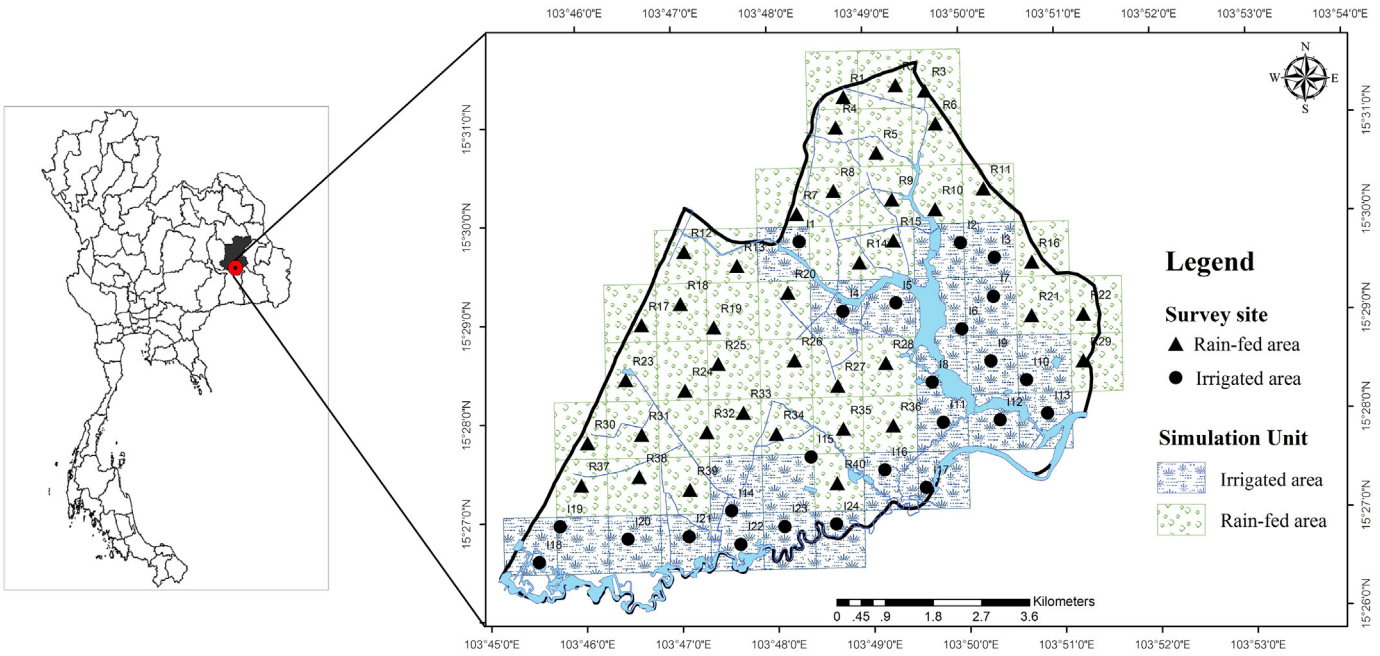

Fig. 1. The location of data collection and simulation unit.

characteristics using a polygonal grid measuring 0.01 × 0.01° in size, and covering ~1 × 1 km. The total area was covered by a total of 64 grid cells, with 24 grid cells in irrigated areas, and 40 grid cells in rain-fed areas (Fig. 1).

2.3.2. Soil sampling and analysis

In a survey of soil nutrient status in Thailand from 2004 to 2008, 13 sites in the study area were sampled by the laboratory of the Office of Science for Land Development, Land Development Department, Ministry of Agriculture, and Cooperatives, Thailand. From the 13 sites in the study area in Thung Kula Sub-district, nine of which were in irrigated areas and four in rain-fed areas, data were collected and the SOC estimated in 2004. In 2014, soil samples were collected again from the same 13 study sites to investigate changes in soil properties and model calibration, and 51 new sites were also investigated for model validation. Soil samples were collected during the dry season after the rice harvest (November 2014). At each site, the soil horizons from 0 to 40 cm in depth were identified based on specific physical features, i.e., color and texture. Three samples (replications) of each soil horizon were then collected. A total of 621 soil samples from 64 sites were collected. Soil profiles were divided into four layers (0–10, 10–20, 20–30, and 30–40 cm). Soil properties of each soil layer in each site were input into soil files of the EPIC model. The soil parameters required for the model and their values are listed in Supplementary Material, Table S1.

2.3.3. Climatic data

The EPIC model requires the following daily climate variables: maximum and minimum air temperature, precipitation, rain days, solar radiation, and relative humidity. In this study, average values of the climatic data were calculated for two separate periods. First, data for the baseline period (1986–2014) was retrieved from the Thai Meteorological Department for calibration and validation of the model. Secondly, the Coupled Model Intercomparison Project Phase 5 (CMIP5) established new climate change scenarios called Representative Concentration Pathways (RCPs) (Taylor et al., 2012) which were used for future climate scenarios. The RCPs are defined by their total radiative forcing pathway (cumulative measure of human emissions of greenhouse gases from all sources expressed in $W\,m^{-2}$) and based on an internally consistent set of socioeconomic assumptions by 2100 (van Vuuren et al., 2011). The data from the National Aeronautics and Space Administration (NASA)-Goddard Institute for Space Studies (GISS) (https://data.giss.nasa.gov/modelforce/ ghgases/) showed that RCP 2.6 assumes a peak in radiative forcing at 2.6 $W\,m^{-2}$ (421.4 ppm CO_2 equivalent) in the year 2100. RCPs 4.5 and 6.0 describe stabilization without overshoot to 4.5 and 6.0 $W\,m^{-2}$ (538.9 and 670.2 ppm CO_2 equivalent), respectively, in the year 2100. Moreover, RCP 8.5 describes a rising radiative forcing pathway leading to 8.5 $W\,m^{-2}$ (936.4 ppm CO_2 equivalent) in the year 2100.

Sixteen GCMs under four future time periods; near future (2020–2039), mid future (2040–2059), far future (2060–2079), and very far future (2080–2099) from CMIP5 of IPCC AR5 were used for climate projection in the study area, namely BCC-CSM1.1, BCC-CSM 1.1-m, CCSM4, CESM1(CAM5), CSIRO-Mk3.6.0, FIO-ESM, GFDL-CM3, GFDL-ESM2M, GISS-E2-H, GISS-E2-R, IPSL-CM5A-MR, MIROC-ESM, MIROC-ESM-CHEM, MIROC5, MRI-CGCM3, and NorESM1-M. Each time period of each GCM model was considered under four RCP scenarios: RCP2.6 (low carbon scenario), RCP4.5 (midlevel carbon scenario), RCP6.0 (midlevel carbon scenario), and RCP8.5 (high carbon scenario). The CMIP5 data were archived at the Climate Change Knowledge Portal of World Bank Group (http://sdwebx.worldbank.org/climateportal/), with a resolution of 1.9° × 1.9° (190 km × 190 km).

However, the spatial resolution of a GCM is too coarse to analyze, so downscaling was conducted separately. Two steps of downscaling were performed to match the spatial resolution of the study area: 1) the monthly data were spatially downscaled into 1 km × 1 km grids by using a kriging method, 2) The linear scaling was used to correct monthly 1 km-data based on the differences between observed and raw GCM data. According to Babur et al. (2016), the temperature is typically corrected with an additive, while precipitation is typically corrected with a multiplier on a monthly basis. Monthly differences in the climate data are acquired using an observed period (1986–2005) of raw GCM and observed data. Therefore, Eqs. (1) and (2) are applied to correct GCM future temperature and precipitation data.

$$T_{fut,d} = T_{GCM,d,fut} + (\overline{T}_{(obs,mon)} - \overline{T}_{(GCM,cont,mon)}) \quad (1)$$

$$P_{fut,d} = P_{GCM,d,fut} \times \left(\frac{\overline{P}_{(obs,mon)}}{\overline{P}_{(GCM,cont,mon)}} \right) \quad (2)$$

where, $T_{fut,d}$ and $P_{fut,d}$ are the corrected temperature and precipitation for the future periods. $T_{GCM,d,fut,}$ and $P_{GCM,d,jut,}$ are the daily temperature and precipitation of the GCM data for future periods. $\overline{T}_{(obs,mon)}$ and $\overline{P}_{(obs,mon)}$ represent the long-term mean monthly temperature and precipitation. $\overline{T}_{(GCM,cont,mon)}$ and $\overline{P}_{(GCM,cont,mon)}$ refer to the long-term monthly mean temperature and precipitation for the control period of the GCM.

2.3.4. Management practice

Management practice data were considered for the two periods. First, the data collected in 2004 was used for model calibration. However, fertilizer application rate data were not available for 2004. Therefore, the trend of fertilizer application rates from 2010 to 2014 was employed using simple linear regression analysis and fitting a linear equation. It was found that the average rate of increase was 1.52 kg ha^{-1} yr^{-1} (1.77% yr^{-1}), which is consistent with Bangkok Bank's (2003) estimate of the Thailand agricultural sector's chemical fertilizer usage from 1995 to 2003. For this eight-year period, the average rate of increase was 1.3% yr^{-1}. Secondly, management data were obtained through field surveys over a five-year period (2010–2014); these data were used for model validation and fixed for each site for model simulation under four RCP climate change scenarios.

Questionnaires were administered at each sampling site to record the crop and management practices of farm owners. Farmers at each of the 64 sites recorded crop and land management data. Rice yields and management practice data (i.e., dates of planting and harvesting; rates of application of fertilizers, manure, pesticides, and irrigation; and field operations performed) were obtained from the surveys in 2014 and from the record books for the standards for good agricultural practices (GAP) of farm owners over the five-year study period (2010–2014), including both rainy and dry seasons. These record books were disseminated to the farmers by the Department of Agricultural Extension, Ministry of Agriculture and Cooperatives, Thailand to record agricultural activities, which helped with the collection of precise operational practice data for this study.

Rice in the study area refers to the major rice crop, which is grown during the rainy season between July and December, and the second rice crop, which is grown during the dry season between January and April of the following year (OAE, 2014). Most rice fields in the study area use rain-fed cultivation, in which rice is grown only once a year because precipitation is a major limiting factor. Farmers in some irrigated areas are able to grow rice twice a year, for both major and second rice crops. Jasmine rice (*Oryza sativa*) is mostly commonly grown in this area. The dominant rice varieties recorded in this study were Khao Dawk Mali 105 (KDML 105), RD 6, and Suphanburi 60. KDML105 and RD 6 are strongly photoperiod sensitive and flower in late October, regardless of sowing time, whereas Suphanburi 60 is a non-photosensitive rice variety. Based on the field survey data, each site was input into the EPIC operation schedule file with the respective farmers' actual management practices specified. Five main types of management operations were incorporated in the EPIC model: seeding/planting, tillage, irrigation, fertilizing, and harvesting. For each type of management operation, the exact date and month, amount and type of fertilizers, crop type, and irrigation conditions were also specified. The main conventional management techniques used in the study area are the following:

First, during the growing period, both major and second rice crops were cultivated using the broadcast method and harvested by machine. The transplanting method was not found at any sites in study areas, thus it was not used in operation schedules in the EPIC model.

Second, for tillage management, conventional tillage to a depth of 20 to 30 cm was performed by machine, with two different situations distinguished between wet and dry soil surface conditions.

Third, after harvesting, farmers applied one of two forms of rice straw and stubble management: incorporation into the soil or burning in the field. The farmers usually burn rice residue after major rice harvesting (dry season) because of the ease and convenience of tillage to prepare for the next crop. Irrigated areas had lower amounts of burned rice residue than rain-fed areas, with averages of 0.071 and 0.141 Mg ha^{-1}, respectively.

Fourth, for water management, continuous flooding and shallow flooding were used for the irrigated and rain-fed areas, respectively. In irrigated areas, the fields were inundated with 10 to 15 cm of standing water throughout the growing period and drained or naturally dried 7 to 10 days before harvesting. In rain-fed areas, the soil was flooded temporarily, depending on rainfall, or water pumping when rain water was unavailable. Therefore, if the field was not in an irrigated area, the irrigation code was set as dryland conditions.

Fifth, the following chemical fertilizer types were found in the study area: 46–0-0, 16–16-8, 16–20–0, 0–0-60, 15–15-15, and 16–8-8. A higher fertilizer application rate was indicated for irrigated areas than for rain-fed areas, with average rates of 320 and 260 kg ha^{-1}, respectively. The total amount of N, P, and K fertilizers were 89, 31, and 15 kg ha^{-1} yr^{-1} for irrigated areas, and 76, 24, and 12 kg ha^{-1} yr^{-1} for rain-fed areas, respectively.

2.4. Sensitivity analysis

A sensitivity analysis was performed to assess the relative importance of crop growth and carbon cycle parameters to model output, as presented in Table 1. The main purpose of sensitivity analysis is to determine the magnitude of changes in the model's response associated with changes in the value of a specified parameter. In this study, the one-factor-at-a-time (OAT) method was used to calculate relative sensitivity indices for rice yields and SOC. A total of five parameters for crop growth and ten parameters for the C cycle were varied by ± 10% of the default model values to assess sensitivity using the equation derived from Liu (2009) below:

$$S = \frac{\Delta Y}{\Delta X}\frac{X}{Y} \tag{3}$$

where S is the sensitivity index of the effect of parameter X_i on Y, Y is the model output (i.e. rice yield and SOC in this study), ΔX is a small change in X, and ΔY is the change in Y in response to the change in X.

Based on Eq. (3), the sensitivity indices for rice yield and SOC are determined as follows:

$$\overline{S}_{yieldi} = \frac{|Yield_{1.1X_i} - Yield_{X_i}| + |Yield_{0.9X_i} - Yield_{X_i}|}{0.2Yield_{X_i}} \tag{4}$$

$$\overline{S}_{SOCi} = \frac{|SOC_{1.1X_i} - SOC_{X_i}| + |SOC_{0.9X_i} - SOC_{X_i}|}{0.2SOC_{X_i}} \tag{5}$$

where $\overline{S}_{yieldi}$ and $\overline{S}_{SOCi}$ are the sensitivity indices of parameter *Xi* for rice yield and SOC, respectively; $Yield_{X_i}$ and SOC_{X_i} are the rice yield and SOC, respectively, simulated by setting all parameters to default values; $Yield_{1.1X_i}$ and $SOC_{1.1X_i}$ are the rice yield and SOC, respectively, simulated by setting all parameters to default values except *Xi*, which is set to 110% of its default value; and $Yield_{0.9X_i}$ and $SOC_{0.9X_i}$ are the rice yield and SOC, respectively, simulated by setting all parameters to default values except *Xi*, which is set to 90% of its default value. The parameters with the highest $\overline{S}_{yieldi}$ and $\overline{S}_{SOCi}$ values are defined as the most sensitive parameters for rice yield and SOC, respectively. The range of sensitivity indices is between 0 (non-sensitive) to 1 (very strongly sensitive); higher values indicate higher sensitivity.

2.5. Model calibration and validation

Calibration and validation are performed by splitting the available observed data into two datasets: one for calibration, and another for validation. Data are most frequently split by time periods (Arnold et al., 2012). Five parameters for crop growth and ten parameters for the C

Table 1
Crop and carbon cycle related default value, suggested range, and calibrated value in EPIC model.

No	Parameter	Symbol	Default value	Suggested range*	Calibrated value
Crop parameters					
1.	Biomass-energy ratio (kg ha^{-1} MJ^{-1} m^2)	WA	25	20–30	25
2.	Harvest index	HI	0.5	0.4–0.5	0.45
3.	Potential heat units (°C)	PHU	1580	1200–2400	1630
4.	Water stress–harvest index	PARM(3)	0.5	0.3–0.7	0.5
5.	SCS curve number index	PARM(42)	1.5	0.5–2.0	1.0
Carbon cycle parameters					
1.	Fraction of humus in the passive pool	FHP	0.0	0.3–0.7	0.6
2.	Fraction of slow C allocated to passive pool	PARM(45)	0.05	0.001–0.05	0.05
3.	Slow humus transformation rate, d^{-1}	PARM(47)	0.000548	0.00041–0.00068	0.000562
4.	Passive humus transformation rate, d^{-1}	PARM(48)	0.000012	0.0000082–0.000015	0.000013
5.	Microbial activity at top soil layer	PARM(51)	1.0	0.1–1.0	1.0
6.	Residue decay tillage coefficient	PARM(52)	10.0	5.0–15.0	14.5
7.	Microbial activity at depth	PARM(53)	0.9	0.8–0.95	0.89
8.	Root growth water use coefficient	PARM(54)	5.0	2.5–7.5	5.7
9.	Root growth water use/depth ratio	PARM(55)	0.5	0.0–1.0	0.8
10.	Root growth depth coefficient	PARM(56)	10.0	5.0–10.0	10.0

* EPIC suggested range.

cycle were selected to calibrate in the EPIC model, as suggested by Wang et al. (2005) and Causarano et al. (2007); these parameters are listed in Table 1. The calibration procedure for the crop growth and SOC modules applied data from the 13 study sites sampled in 2004. Rice yields were measured values collected from the Agricultural Statistics of Thailand report for 2004, which was generated by the Office of Agricultural Economics (OAE), Ministry of Agriculture and Cooperatives (MOAC), Thailand. The SOC measurements were collected by the Land Development Department of Thailand in 2004. A total of 2000 parameter sets were generated for crop and carbon cycle parameters using the SIMLAB software (version 2.2.1) from the given ranges and distribution specified in Table 1. The model validation procedure focused on the measured values at all sites (64 sites), which were collected over five years (2010–2014) for rice yield, and in 2014 for SOC.

2.6. Model performance evaluation

Model calibration and validation were evaluated using two criteria: the coefficient of determination (R^2), and the Nash–Sutcliffe model efficiency coefficient (*Ens*) (Nash and Sutcliffe, 1970). In this study, the model performance was considered satisfactory if $R^2 > 0.5$ (Santhi et al., 2001) and *Ens* ≥ 0.60 (Wang et al., 2012). The maximum R^2 and *Ens* were selected by the parameterization scheme as the optimal parameter set.

R^2 is defined as:

$$R^2 = \left\{ \frac{\sum_{i=1}^{n} (M_i - \overline{M_i})(S_i - \overline{S_i})}{[\sum_{i=1}^{n} (M_i - \overline{M_i})^2]^{0.5} [\sum_{i=1}^{n} (S_i - \overline{S_i})^2]^{0.5}} \right\} \quad (6)$$

where S_i and M_i are the simulated and measured values, respectively, at site *i*. $\overline{M}$ and $\overline{S}$ are the means of the measured and simulated values, respectively. The range of R^2 is between 0 (no correlation) and 1 (perfect fit).

Ens is defined as:

$$Ens = 1 - \frac{\sum_{i=1}^{n} (S_i - M_i)^2}{\sum_{i=1}^{n} (M_i - \overline{M})^2} \quad (7)$$

where S_i and M_i are the simulated and measured values, respectively, at site *i*. The range of *Ens* lies between 1 (perfect fit) and $-\infty$. A negative value indicates that the mean value of the observed time series would have been a better predictor than the model.

2.7. Climate change impact assessment

This portion of the evaluation consists of analyzing climate data to understand the projected changes in climate with respect to the baseline period (1986–2014) and the EPIC model simulation to assess the possible impacts on rice yield and SOC over the four RCP scenarios (RCPs 2.6, 4.5, 6.0, and 8.5) and four future time periods; near future (2020–2039), mid future (2040–2059), far future (2060–2079), and very far future (2080–2099). Management practices and parameters for the simulation periods were fixed as those of the baseline period for each site. Changes in key climate change indicators (temperature and precipitation), rice yield, and SOC were analyzed by subtracting the output values under the climate change scenarios from the baseline values, and by estimating the percentage of change.

2.8. Evaluating the effects of CO_2, temperature and precipitation on rice yield and SOC

There is a complexity of climate change variables that may drive the changes of rice yield and SOC with different magnitudes, trends, and durations. To clarify the dominant drivers, this study evaluated the response of rice yield and SOC by inputting the changing of CO_2 concentrations, maximum and minimum temperatures, and precipitation separately, while other input data were constant at baseline periods. For example, when the CO_2 effect on rice yield was evaluated, all input data were fixed at the baseline condition, with the exception of four levels of CO_2 concentration under four RCP scenarios, which were inputted and simulated by using the OAT method. The outputs were compared with the baseline.

2.9. Statistical analysis

Statistical analyses of the data were performed using SPSS (version 20.0, USA). Mean and standard deviation (SD) values were used to represent rice yields and SOC for different areas and periods. Differences in rice yield and SOC between the baseline period (1986–2014) and the four future time periods under the four RCP scenarios were analyzed with *t*-tests and least significant difference (LSD) tests ($p < 0.05$). A simple linear regression analysis was used to find the relationships between measured and simulated values by fitting linear equations.

Table 2
Model evaluation statistics for calibration and validation procedures.

		Minimum	Maximum	Mean ± SD	Model performance	
					R^2	*Ens*
Model calibration procedure (n = 13)						
Rice yield (Mg ha^{-1} yr^{-1})	Measured	1.8	3.8	2.9 ± 0.7	0.66	0.62
	Simulated	1.7	4.3	3.1 ± 0.8		
SOC (Mg C ha^{-1})	Measured	14.2	111.5	48.1 ± 28.5	0.71	0.68
	Simulated	15.9	74.8	37.8 ± 21.1		
Model validation procedure (all sites, n = 64)						
Rice yield (Mg ha^{-1} yr^{-1})	Measured	1.3	4.9	2.6 ± 0.9	0.78	0.75
	Simulated	1.1	4.7	2.7 ± 0.8		
SOC (Mg C ha^{-1})	Measured	3.8	129.9	37.7 ± 32.1	0.88	0.83
	Simulated	5.6	114.5	38.0 ± 30.3		

3. Results and discussion

3.1. Model calibration

Model calibration was performed to compare the simulated rice yields and SOC with measured values for 13 sites. The results show that rice yields varied from 1.8 to 3.8 Mg ha^{-1} yr^{-1} and 1.7 to 4.3 Mg ha^{-1} yr^{-1} for the measured and simulated values, respectively. The average rice yields were 2.9 and 3.1 Mg ha^{-1} yr^{-1}, with standard deviations of 0.7 and 0.8 Mg ha^{-1} yr^{-1} for measured and simulated values, respectively (Table 2). The ranges of SOC values were 14.2–111.5 Mg C ha^{-1} and 15.9–74.8 Mg C ha^{-1} for the measured and simulated values, respectively. The average of the SOC values were 48.1 and 37.8 Mg C ha^{-1}, with standard deviations of 28.5 and 21.1 Mg C ha^{-1}, for the measured and simulated values, respectively (Table 2).

For the calibration procedure, the rice yield simulation R^2 and *Ens* values were 0.66 and 0.62, respectively, and the SOC R^2 and *Ens* values were 0.71 and 0.68, respectively (Table 2). The measured and simulated rice yield and SOC values were distributed near the line $y = x$, and the r values were 0.7128 and 0.7708, respectively (Figs. 2 and 3). These findings indicate that the model was satisfactorily consistent with the results of visual evaluations and the best-fitting parameterization. For the sensitivity analysis, higher values indicate a higher sensitivity. These results show that HI is the most sensitive parameter for rice yield, followed by WA, PHU, PARM(42), and PARM(3), with sensitivity indices of 0.911, 0.665, 0.515, 0.218, and 0.232, respectively. These findings are consistent with those of Liu (2009), which indicate that HI is the most sensitive parameter for rice in Asia, followed by WA, PARM (42), PARM(3), and PHU, with sensitivity indices of 0.997, 0.485, 0.342, 0.334, and 0.318, respectively. This similarity is because the potential yields in the EPIC model are based on the accumulation of actual aboveground biomass and harvest indices, which are a function of the crop/variety and water stress in defined crop development stages (Gaiser et al., 2010). The highest sensitivity parameter for SOC is FHP, followed by PARM(47), PARM(51), PARM(55), PARM(54), PARM(45), PARM(52), PARM(56), PARM(53), and PARM(48), with sensitivity indices of 0.512, 0.075, 0.062, 0.033, 0.022, 0.021, 0.018, 0.013, 0.011, and 0.010, respectively. These results support those of Causarano et al. (2007), who reported that FHP was the most influential parameter for microbial biomass carbon (MBC) and particulate organic carbon (POC).

3.2. Model validation

The measured and simulated rice yield and SOC values were distributed near the line $y = x$, and the r values were 0.706 and 0.797, respectively (Figs. 2 and 3). The model performance of the validation procedure for rice yield was evaluated based on the R^2 and *Ens* values, which were 0.78 and 0.75, respectively. For SOC simulation, the statistical performance values were $R^2 = 0.88$ and *Ens* = 0.83, as shown in Table 2. Overall, the validation and reliability of the EPIC model are acceptable and indicate good predictive capability, as indicated by the

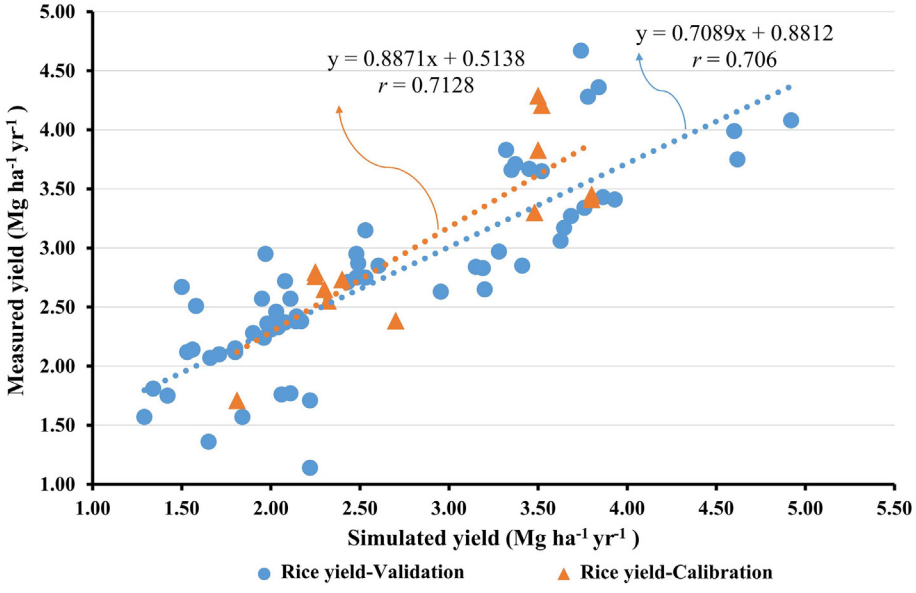

Fig. 2. Result of rice yield calibration and validation of EPIC model.

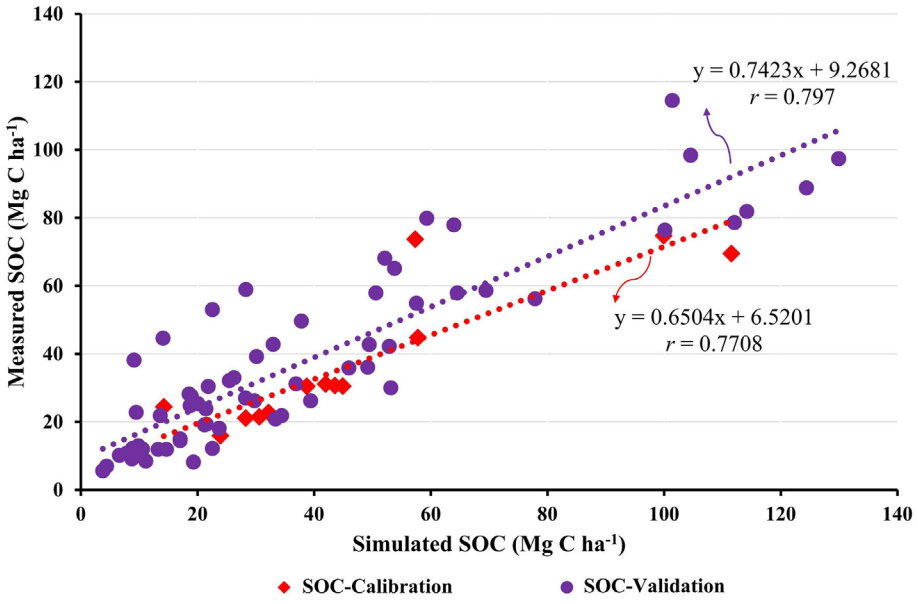

Fig. 3. Result of SOC calibration and validation of EPIC model.

values of $R^2 > 0.50$ and *Ens* > 0.60 for both rice yield and SOC. In this study, overestimation by the EPIC model was found for both rice yield and SOC (Table 2). These results support those of Guerra et al. (2004), who pointed out that this model tends to overestimate at low yields, especially under water-stress conditions. Similarly, Izaurralde et al. (2006) reported that the EPIC model overpredicts at low SOC values and under predicts at high SOC values. Gaiser et al. (2010) reported that the performance of the EPIC model was best for slightly acidic soils ($R^2 = 0.85$) and poorest for strongly acidic soils with high aluminum saturation ($R^2 = 0.40$). In particular, when extremely acidic soils were associated with semi-arid conditions and with high precipitation variability, then the model strongly overestimated crop yields. These findings support the overestimation of the EPIC model detected in our study area, where low pH values (3.86–6.66) are measured in surface soils to 40 cm depth and precipitation is highly variable for the whole year (Table 4).

The average simulated and measured rice yields were 2.6 and 2.7 Mg ha^{-1} yr^{-1}, while average values of 37.7 and 38.0 Mg C ha^{-1} were found for the simulated and measured SOC, respectively. These results indicate that the EPIC model tends to overestimate both rice yield and SOC, with average overestimations of 0.05 Mg ha^{-1} yr^{-1} and 0.28 Mg C ha^{-1}, respectively.

3.3. Changes in future climate scenario

Comparison of baseline and CMIP5 climate data, including minimum and maximum temperature, and precipitation, are presented in Fig. 4. In Roi Et province, an increase in the ensemble average of future climate data was detected under all climate scenarios, compared with the baseline. The average minimum temperature was predicted to increase by 22.3 to 25.1 °C under RCP2.6 and RCP 8.5, respectively, while the baseline was 21.8 °C. Similarly, an increasing trend was detected for average maximum temperature, reporting that 33.2 to 36.2 °C will occur under RCP2.6 and RCP 8.5, respectively, while the baseline was 32.6 °C. The average annual precipitation will tend to rise, with values of 1495.3 to 1629.1 mm under RCP2.6 and RCP 8.5, respectively, compared to 1375.7 mm, which was recorded as the baseline.

All the future climate scenarios show temperatures and precipitation increasing over the next 80 years. The RCP8.5 scenario shows the highest average temperatures and precipitation. Downing (1992), Rosenzweig and Iglesis (1994), Furuya and Koyama (2005), and Aggarwal et al. (2010) also reported that both the maximum and minimum temperatures, as well as average temperatures, in Asia are increasing, and average precipitation may also increase.

The average monthly mean temperature change will be the highest during April and May under all climate scenarios. However, the increasing temperature will not occur in every month. The temperature will tend to decline from the baseline by about 0.2–1.2 °C during November, December, January, and February. Overall, the precipitation amount tends to increase at all periods of time and all climate scenarios, especially in June, July, August, October, November, and December. Meanwhile, it tends to reduce in other months in the CMIP5 climate data (see in Supplementary Material, Tables S2-S5).

3.4. The effect of CO_2 alone on SOC

When all climate variables were assigned as baseline condition, the levels of CO_2 concentration were changed following RCP scenarios. The simulation revealed that the effect of CO_2 will cause increasing SOC sequestration at all the sites by +32.0%, which under RCP8.5 will bring the highest increased SOC, followed by RCP6.0, RCP4.5, and RCP2.6 with values of +29.1%, +20.0%, and +8.7%, respectively (Table 3). The importance of SOC sequestration is that it increases the SOC pool, which can reduce the CO_2 concentration in the atmosphere (Ringius, 2002). The simulation showed the positive effect of elevated CO_2 on SOC increase, consistent with Li et al. (2011) who used the CENTURY model to simulate the effects of climate change and elevated CO_2 on SOC in an Alpine Steppe. Their simulation showed that under the CO_2 doubling scenario, SOC increased by 12.87%, compared with the unchanged CO_2 scenario. This is because increasing atmospheric CO_2 concentrations can increase the photosynthetic rate of plants, improve water use efficiency and nutrient use efficiency (Owensby et al., 1993), which can reduce soil water loss through transpiration (van Groenigen et al., 2011). These lead to increased plant productivity, plant litter, and roots, resulting in higher soil C sequestration and SOC content (Ojima et al., 1993; Gifford, 1994; Ni, 2001).

On the other hand, Nie et al. (2013) found that elevated CO_2 can increase the ability of microbes to decompose SOM and stimulate the activity of enzymes associated with decomposition processes (Carney et al., 2007), which lead to loss of SOC through releasing CO_2 into the atmospheric. Moreover, Van Groenigen et al. (2017) strongly suggested that faster decomposition of new C (plant-derived inputs can

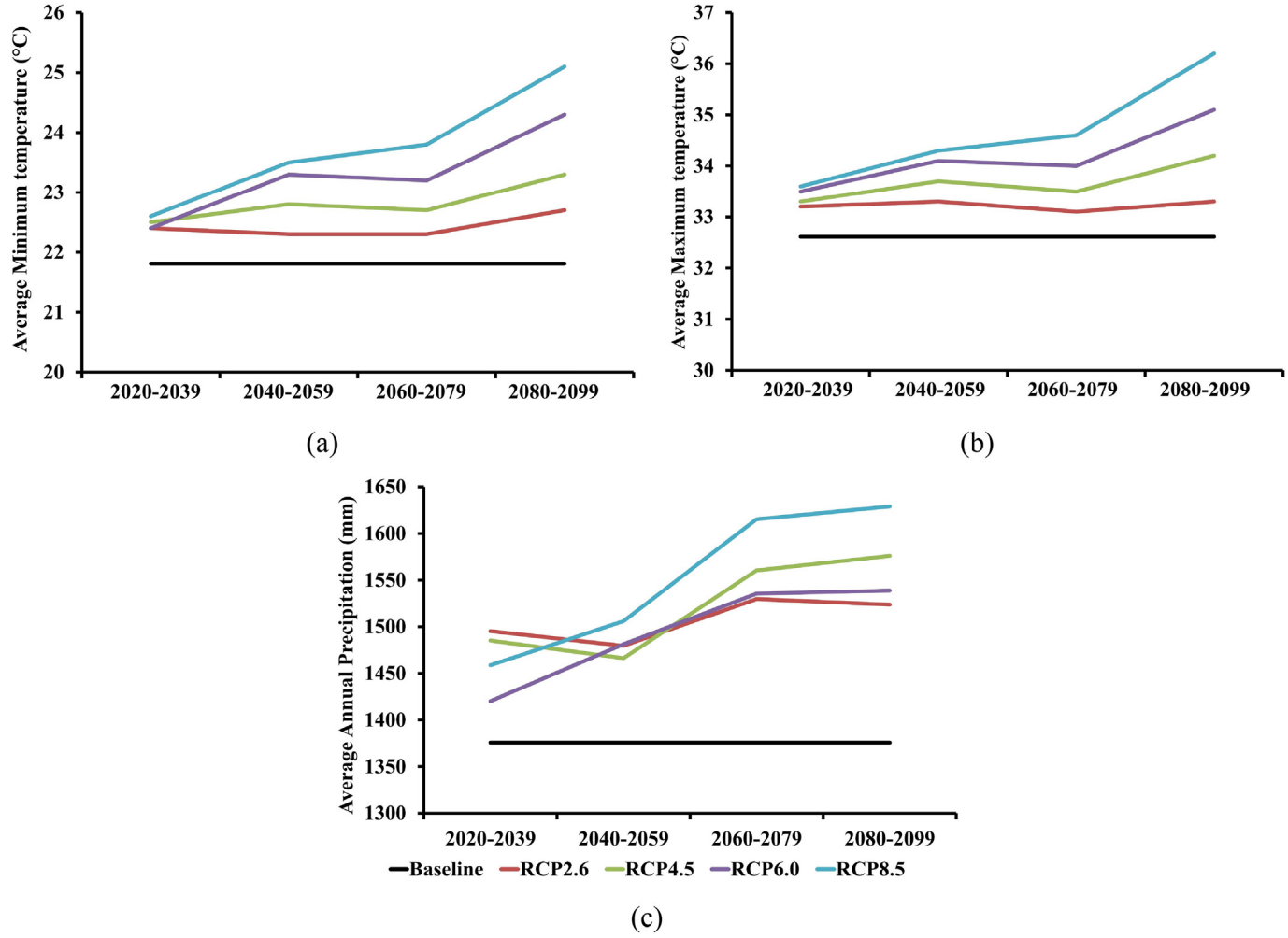

Fig. 4. The average CMIP5 climate data: (a) minimum temperature, (b) maximum temperature, (c) precipitation.

accumulate in the soil and become part of the soil C pool) under elevated CO_2 negated the higher soil C input rates, resulting in longer-term soil C storage being limited. It is important to point out that there are other principal factors controlling SOC dynamics, which could have significant impacts on SOC sequestration, especially precipitation and temperature (Lal, 2003, 2008).

3.5. The effect of precipitation alone on SOC

Increasing precipitation resulted in a loss of SOC sequestration at all sites by −30.0%, −27.1%, −21.1%, and − 18.6% under RCP8.5, RCP6.0, RCP4.5, and RCP2.6, respectively (Table 3). This is because precipitation influences soil moisture and hydrological processes, which are important for controlling SOC content and its dynamics (Heisler and Weltzin, 2006; Aanderud et al., 2010) and could also be a modifier of the magnitude of the C sink (Goebel et al., 2011). These results are consistent with the study of Meier and Leuschner (2010), who found that SOC decreased by about 25% from stands with annual precipitation > 900 mm yr^{-1} to those with precipitation < 600 mm yr^{-1}, and concluded that SOC reduction is mainly due to higher decomposition rates, resulting from rising precipitation-increased microbial activity (Alvarez and Alvarez, 2001; Zhang et al., 2004).

3.6. The effect of temperature alone on SOC

When changing the temperature according to RCP scenarios while keeping other factors at the baseline condition, it was found that expected changes in maximum and minimum temperatures have similar negative impacts on SOC. Rising maximum temperatures result in an 8.8% reduction in SOC at all sites under RCP8.5, and by −5.8%, −4.3%, and −1.8% in the RCP6.0, RCP4.5, and RCP2.6 scenarios, respectively. Likewise, a 4.1% reduction in SOC was detected under RCP8.5 at all sites for the effect of minimum temperature. However, changing the maximum temperature is likely to have a greater impact on SOC than the effect of the minimum temperature (Table 3). These findings are consistent with those of Curiel et al. (2004), Conant et al. (2008), Zhou et al. (2009) and Thomas et al., 2011, who confirmed that an increase in air temperature causes an increase in soil respiration and enhances SOC decomposition because of increased microbial activity (Smith et al., 2005; Gottschalk et al., 2012).

3.7. The combined effect of CO_2, precipitation and temperature on SOC

Under four RCP scenarios, SOC decreased significantly in all time periods compared to the baseline SOC. The largest decrease in SOC was found to be −32.0%, under RCP8.5 in the very far future, followed by RCP4.5, RCP6.0, and RCP2.6 with decreases of −31.0%, −16.0%, and −16.0%, respectively. On the other hand, there is no statistically significant difference between SOC change in the near future and the baseline. The results indicate that SOC changes in the near future are slightly increased by +1.6%, +1.5%, +0.8% under RCP2.6, RCP6.0, and RCP4.5, and that under RCP8.5 it tends to decrease by −3.2%. The results also showed that the decreases of SOC in rain-fed areas were higher than those in irrigated areas compared to the baseline, and that

Table 3
The response of SOC (Mg C ha^{-1}) on the effect of CO_2, precipitation, maximum and minimum temperature.

		Baseline	CMIP5 climate data			
			RCP2.6	RCP4.5	RCP6.0	RCP8.5
Effect of CO_2						
Irrigated	SOC	43.5	47.6	52.2	55.9	57.2
	% of change	–	9.5	20.1	28.6	31.6
Rain-fed	SOC	34.7	37.3	41.5	44.9	45.9
	% of change	–	7.4	19.7	29.5	32.4
All sites	SOC	38.0	41.3	45.6	49.1	50.2
	% of change	–	8.7	20.0	29.1	32.0
Effect of precipitation						
Irrigated	SOC	43.5	35.4	34.6	31.5	31.1
	% of change	–	−18.7	−20.5	−27.7	−28.5
Rain-fed	SOC	34.7	28.3	27.2	25.5	23.8
	% of change	–	−18.4	−21.7	−26.4	−31.4
All sites	SOC	38.0	31.0	30.0	27.7	26.6
	% of change	–	−18.6	−21.1	−27.1	−30.0
Effect of maximum temperature						
Irrigated	SOC	43.5	42.7	41.6	40.8	39.8
	% of change	–	−1.8	−4.4	−6.1	−8.6
Rain-fed	SOC	34.7	34.1	33.2	32.8	31.6
	% of change	–	−1.8	−4.3	−5.5	−8.9
All sites	SOC	38.0	37.3	36.3	35.8	34.7
	% of change	–	−1.8	−4.3	−5.8	−8.8
Effect of minimum temperature						
Irrigated	SOC	43.5	43.1	43.0	42.8	41.7
	% of change	–	−0.9	−1.2	−1.5	−4.2
Rain-fed	SOC	34.7	34.1	33.9	33.8	33.3
	% of change	–	−1.6	−2.3	−2.5	−3.9
All sites	SOC	38.0	37.5	37.3	37.2	36.5
	% of change	–	−1.3	−1.8	−2.0	−4.1

the largest decrease in SOC was detected under RCP8.5 in the very far future (Fig. 5). These findings are in line with a previous study in Roi Et province by Arunrat (2017), who used the EPIC model to project the SOC changes under the combined effects of CO_2, precipitation, and temperature. Their simulation showed that climate change decreases SOC sequestration because of rises in temperature and precipitation that accelerate SOC decomposition.

According to the results shown in Table 3, increases in temperature and precipitation are the two main factors that cause SOC reduction under the future climate in this area, with precipitation being the most important, and negating the enrichment of CO_2 fertilization. This phenomenon is consistent with the study by Hobley and Wilson (2016), who concluded that precipitation is the most important factor influencing SOC dynamics in the soils of eastern Australia, compared with other climate variables. Dintwe et al. (2014) showed that the precipitation was strongly related to SOC storage in the Kalahari, thereby Dintwe and Okin (2018) hypothesized that changes in precipitation will generate the strongest response in SOC storage, rather than temperature or CO_2 concentrations, whereas the increase in soil temperature opposes the effect of increased CO_2, leading to lower SOC storage overall.

Much greater decreases in SOC are estimated under the RCP8.5 scenario than other scenarios (Fig. 5). Not surprisingly, this difference is because temperatures and precipitation under the RCP8.5 scenario rose much higher than those under the other scenarios (Fig. 4), which results in increased C release and a decreased C reservoir. This indicates that the decay rates of the residues are higher than the plant residues added into the soil. It is necessary to note that even though SOC at a depth of 40 cm was analyzed in this area, it is the closest and most rapid interaction with the atmosphere (Parton et al., 2010) and very important for understanding the interactions between the soil and the atmosphere (Dintwe and Okin, 2018).

3.8. The effect of CO_2 alone on rice yield

The findings of this study show that when the CO_2 effect was accounted for, rice yields increased by +5.6%, +16.4%, and +32.9% under the RCP2.6, RCP4.5, and RCP6.0 scenarios, respectively. Conversely, elevated CO_2 under RCP8.5 resulted in a rice yield decrease of −2.9% at all sites (Table 4). This is because the elevated CO_2 concentration in the atmosphere may cause direct effects on plants in the form of CO_2 fertilization (McGrath and Lobell, 2013), reduction of the stomatal conductance, and enhancement of the plants' water-use efficiency (Acock, 1990; Rosenberg, 1981). A large number of previous studies have indicated that carbon fertilizer effects are different for C3 (rice) and C4 plants as a result of photosynthetic impacts on productivity gain, which could lead to a higher yield of C3 plants than C4 plants (Kimball et al., 2002; Caylor and Shugart, 2004; Long et al., 2005; Thomson et al., 2005; Högy and Fangmeier, Hogy and Fangmeier, 2008; Shimono et al., 2009; Bocchiola, 2015). Based on observations from many experimental studies, Patterson and Flint (1980), Kimball (1983), and Acock (1990) reported that a doubling of the CO_2 concentration may cause the average yield to increase by 33% to 34% for C3 plants and 14% for C4 plants. From a modeling perspective, research by Erda et al. (2004, 2005) using the PRECIS model for China showed that rice yields are higher under the A2 scenario (549 ppm CO_2 concentration) than under the B2 scenario (488 ppm CO_2 concentration). Lin et al. (2005) used the PRECIS regional climate model and the CERES crop model to analyze the impacts of climate change and CO_2 fertilization on crop productivity for both the A2 and B2 scenarios and found highly variable results for wheat, corn, and rice depending on the scenario and irrigation practices used. This is because the different levels of CO_2 directly affect the rice yields. The continuously increasing levels of CO_2 also cause yields and biomass to increase by 5–15%. Rice yields at 550 ppm CO_2 are therefore greater than those at 450 ppm CO_2. Increasing levels of CO_2 may cause negative effects on the germination of rice seeds and decrease stomatal aperture sizes but may enhance photosynthetic activity (Mott, 1988). This finding is consistent with Bhattarai et al. (2017), who used the EPIC model to project corn and soybean yields under climate change during

Time period	SOC change in irrigated area (%)				SOC change in rain-fed area (%)				SOC change in all sites (%)			
	RCP2.6	RCP4.5	RCP6.0	RCP8.5	RCP2.6	RCP4.5	RCP6.0	RCP8.5	RCP2.6	RCP4.5	RCP6.0	RCP8.5
Baseline (Mg C ha^{-1})	43.5±33.4				34.7±28.1				38.0±30.3			
2020-2039	0.5	0.7	2.0	1.8	-7.5	-7.3	-6.0	-6.2	1.6	0.8	1.5	-3.2
2040-2059	0.9	1.2	0.3	-2.0	-7.1	-6.8	-7.7	-10.0*	-4.1	-3.8	-4.7	-7.0*
2060-2079	-3.0	-12.0*	-5.0	-24.0**	-11.0*	-20.0**	-13.0*	-32.0**	-13.0*	-22.0**	-13.0*	-29.0**
2080-2099	-4.0	-18.0*	-7.0	-27.0**	-12.0*	-26.0**	-15.0*	-35.0**	-16.0**	-31.0**	-16.0**	-32.0**

Fig. 5. Simulation the effect of precipitation, temperature and CO_2 on SOC change under RCP2.6, RCP4.5, RCP6.0, and RCP8.0 climate change scenarios. *, ** = Significant at 5% and 1%, between baseline and four long-term periods (2020–2039, 2040–2059, 2060–2079, and 2080–2099) under RCP2.6, RCP4.5, RCP6.0, and RCP8.0 climate change scenarios.

Table 4
The response of rice yield (Mg ha^{-1} yr^{-1}) on the effect of CO_2, precipitation, maximum and minimum temperature.

		Baseline	CMIP5 climate data			
			RCP2.6	RCP4.5	RCP6.0	RCP8.5
Effect of CO_2						
Irrigated	Rice yield	2.9	3.1	3.3	4.0	2.8
	% of change	–	5.8	13.6	37.1	−2.7
Rain-fed	Rice yield	2.4	2.5	2.8	3.1	2.3
	% of change	–	4.3	16.2	28.7	−3.2
All sites	Rice yield	2.7	2.7	3.0	3.5	2.5
	% of change	–	5.6	16.4	32.9	−2.9
Effect of precipitation						
Irrigated	Rice yield	2.9	3.3	3.7	3.6	3.9
	% of change	–	12.5	28.4	25.2	35.2
Rain-fed	Rice yield	2.4	2.8	3.1	3.0	3.3
	% of change	–	15.3	30.2	26.4	38.4
All sites	Rice yield	2.7	3.0	3.4	3.3	3.6
	% of change	–	13.9	29.3	25.8	36.8
Effect of maximum temperature						
Irrigated	Rice yield	2.9	2.9	2.8	2.9	2.8
	% of change	–	−0.7	−1.8	−1.6	−4.9
Rain-fed	Rice yield	2.4	2.4	2.3	2.3	2.3
	% of change	–	−1.4	−3.7	−2.9	−4.6
All sites	Rice yield	2.7	2.6	2.5	2.5	2.5
	% of change	–	−1.2	−2.4	−2.2	−4.75
Effect of minimum temperature						
Irrigated	Rice yield	2.9	2.7	2.7	2.7	2.6
	% of change	–	−5.5	−7.6	−8.4	−9.7
Rain-fed	Rice yield	2.4	2.3	2.2	2.2	2.2
	% of change	–	−6.2	−8.5	−9.7	−9.4
All sites	Rice yield	2.7	2.4	2.4	2.4	2.4
	% of change	–	−5.8	−8.1	−9.1	−9.6

2015–2099 in the US. Their simulation showed that the carbon fertilizer effects on soybean, a C3 plant, increased in yield by 2% to 20%, while both corn and soybean yields will decline under the high carbon scenario 2080–2099. This may be because the excessive elevated CO_2 led to a decrease in the photosynthetic capacity by reducing the total nitrogen and chlorophyll contents in the leaves (Nakano et al., 1997).

3.9. The effect of precipitation alone on rice yield

Increased precipitation can enhance crop growth and production, and result in rice yield increases of +13.9%, +29.3%, +25.8%, and +36.8% at all sites under the RCP2.6, RCP4.5, RCP6.0, and RCP8.5 scenarios, respectively. Higher rates of increase are found in rain-fed areas than in irrigated areas in all periods and under all future climate scenarios (Table 4). This indicates that future climate scenarios may evoke greater benefits for rice grown in rain-fed areas than in irrigated areas because increasing amounts of precipitation can reduce water stress in rain-fed areas by increasing soil available water and enhancing crop growth, which are accompanied by higher yields (Agele et al., 2011). Furthermore, as indicated by Salvador Sanchis et al. (2008), soil available water and distribution may respond rapidly to climate change, especially drought events; therefore, enhancing water infiltration and available water in soil may help mitigate the impacts of severe drought events in rain-fed areas. Shen et al. (2011) showed that irrigated rice generally has higher rice yields in the middle and lower reaches of the Yangtze River valley compared to the rain-fed rice, because irrigated rice is less affected by climate change, and irrigation can relieve water stress for rice growing in the northern region of the Yangtze River valley. Their results show that under irrigation conditions, rice growth is not influenced by precipitation, whereas rain-fed rice is susceptible to the temporal and spatial variation of precipitation. These findings support the result that future climate change scenarios could have positive impacts on rice yield in northeast Thailand in the next 80 years, especially in rain-fed areas, because rice yields in the study area vary depending on the distribution of precipitation during the growing season.

3.10. The effect of temperature alone on rice yield

The negative effect of both maximum and minimum temperatures on rice yield were detected when other variables were kept at the baseline condition. An increased maximum temperature will decrease rice yield by −1.2%, −2.4%, −2.2%, and −4.75% under the RCP2.6, RCP4.5, RCP6.0, and RCP8.5 scenarios, respectively, at all the sites. Furthermore, increasing minimum temperatures could reduce rice yield by more than rising maximum temperatures, which will decline by −5.8%, −8.1%, −9.1%, and −9.6% under the RCP2.6, RCP4.5, RCP6.0, and RCP8.5 scenarios, respectively, at all sites (Table 4). This is because rising maximum and minimum temperatures under future climate exceed the optimal temperature for crop growth, which results in crop yield reduction. Similarly, Porter and Gawith (1999) and Ottman et al. (2012) reported that temperature increase has the most likely negative impact on crop yields. The reasons behind this phenomenon can be explained by the studies of Asseng et al. (2011), Nelson et al. (2014), and Zhao et al. (2016) which indicated that increasing temperature can increase atmospheric water demand, which could lead to water stress, afterward reducing soil moisture and decreasing yield. In addition, Tack et al. (2015) and Lesk et al. (2016) mentioned that an indirect impact of rising temperature is more frequent heat waves, which benefit weeds, pests, and diseases.

3.11. The combined effect of CO_2, precipitation, and temperature on rice yield

Overall, rice yields at all sites under future climate scenarios tend to increase significantly compared to the baseline yield by +0.7% (RCP8.5: 2060–2079) to +18.8% (RCP6.0: 2080–2099), with the exception of 2080–2099 under RCP8.5, which results in a decline in rice yield by −8.4% ($p < 0.01$ and 0.05). The average baseline rice yield was 2.7 Mg ha^{-1} yr^{-1} at all sites, while the average values of 2.9 and 2.4 Mg ha^{-1} yr^{-1} were the baseline yield in irrigated and rain-fed areas, respectively. Under future climate scenarios, rice yield will be increased by +3.2% (RCP2.6: 2020–2039) to +18.8% (RCP6.0: 2080–2099), whereas in 2060–2079 and 2080–2099 under RCP8.5 there will be a decrease in rice yield by −7.0% and −11.2% in irrigated areas, respectively. Beneficially, future climate change will bring an increase in rice yield for rain-fed areas in all periods and future climate scenarios by +2.6% (RCP8.5: 2080–2099) to +22.7% (RCP6.0: 2080–2099) (Fig. 6). These results are consistent with a previous study by Arunrat (2017), who used the EPIC model to simulate the rice yield changes under the combined effects of CO_2, precipitation, and temperature in Roi Et province. Results showed that the average rice yield under the A2 scenario were higher than those under the B2 scenario. This is because increasing temperature, CO_2 concentration, and precipitation patterns were detected in this area, which are the general important factors of climate with pronounced impacts on crops (Jinger et al., 2017). Similar findings were presented by Tao et al. (2006 and 2014), who reported that crop production would increase by 7.9–11.9% when rising CO_2 concentration was not considered, whereas productivity would increase by 31.3–44.5% after rising CO_2 was input into the model.

However, the findings of this study show that the precipitation is the most important factor for rice yield because it was found to produce the highest percentage of rice yield change in this area, followed by the effects of CO_2 concentration and temperature. Interestingly, although rising temperature will slightly reduce the rice yield, its impact will reduce by a large amount with increased CO_2 concentration and precipitation (Table 4). This is in line with Akpalu et al. (2008), who found that increased temperature and precipitation have a positive effect on

Time period	Rice yield change in irrigated area (%)				Rice yield change in rain-fed area (%)				Rice yield change in all sites (%)			
	RCP2.6	RCP4.5	RCP6.0	RCP8.5	RCP2.6	RCP4.5	RCP6.0	RCP8.5	RCP2.6	RCP4.5	RCP6.0	RCP8.5
Baseline (Mg ha^{-1} yr^{-1})	2.9±1.1				2.4±0.7				2.7±0.8			
2020-2039	3.2	6.3	6.9*	7.7*	7.1*	10.2*	10.8	11.6*	4.7	8.0*	8.5*	9.6*
2040-2059	4.9	6.9	7.3*	8.2*	8.8*	10.8*	11.2*	12.1*	5.5	8.5*	9.2*	10.2**
2060-2079	5.6	10.0*	10.8*	-7.0*	9.5*	13.9*	14.7*	8.0*	6.9*	10.2**	11.8**	0.7
2080-2099	16.5**	18.5**	18.8**	-11.2**	20.4**	22.4**	22.7**	2.6	15.0**	17.8**	18.4**	-8.4*

Fig. 6. Simulation the effect of precipitation, temperature and CO_2 on rice yield change under RCP2.6, RCP4.5, RCP6.0, and RCP8.0 climate change scenarios. *, ** = Significant at 5% and 1%, between baseline and four long-term periods (2020–2039, 2040–2059, 2060–2079, and 2080–2099) under RCP2.6, RCP4.5, RCP6.0, and RCP8.0 climate change scenarios.

maize yield, and that precipitation is more important than the temperature for maize yield in the Limpopo Basin of South Africa.

It is also important to note that as the results for SOC presented here were decomposed influencing by increased precipitation under the future climate, resulting in a large increase in rice yield in this area. This is because increased precipitation accelerated organic matter decomposition rates and causes the rapid release of nutrients into the soil (Brady and Weil, 1999), which may increase N availability (Mack et al., 2004; Schaeffer et al., 2013) and lead to increased yields (Kant et al., 2012; Xu et al., 2013).

4. Conclusions

The EPIC model performance was satisfactory and acceptable; the model therefore provided good predictions of rice yields and changes in SOC under future climate conditions in rice paddy fields. All the future climate scenarios show temperatures and precipitation increasing over the next 80 years. Climate change will impact rice yields positively, which will benefit farmers, especially in rain-fed areas. The findings of this study revealed that the precipitation is the most important factor for rice yield, and increased precipitation was detected as being responsible for the highest percentage of rice yield increase in this area. Although rising temperatures will slightly reduce rice yields, the impact will be negated by large amounts by increased CO_2 concentration and precipitation. SOC sequestration, on the other hand, will decrease under the future climate scenarios. It is strongly implied that increasing temperature and precipitation are two main factors that cause SOC reduction under the future climate in this area, with precipitation being the most important and negating the enrichment of CO_2 fertilization. It is important to note that the result of SOC was decomposed, resulting in large increase of rice yield in this area. This is because rises in temperature and precipitation accelerate SOC decomposition, which may increase nitrogen availability to the soil and increase yield. These findings contribute to understanding the consequences of long-term climate change, which is essential for agricultural policy-making and the selection of mitigation strategies.

Acknowledgments

This article was supported by the research grant nr. RDG6020014. The authors thank the reviewers for providing helpful comments to improve the manuscript.

Appendix A. Supplementary data

Supplementary data to this article can be found online at https://doi.org/10.1016/j.agsy.2018.04.001.

References

Aanderud, Z.T., Richards, J.H., Svejcar, T., 2010. A shift in seasonal rainfall reduces soil organic carbon storage in a cold desert. Ecosystems 13, 673–682.

Acock, B., 1990. Effects of carbon dioxide on photosynthesis plant growth and other processes 1. In: Kimball, B.A. (Ed.), Impact of Carbon Dioxide, Trace Gases, and Climate Change on Global Agriculture. American Society of Agronomy, Crop Science Society of America, and Soil Science Society of America, Madison, WI, pp. 45–60.

Adejuwon, J.O., 2005. Food crop production in Nigeria. I. Present effects of climate variability. Clim. Res. 30, 53–60.

Agele, S.O., Iremiren, G.O., Ojeniyi, S.O., 2011. Evapotranspiration Water use efficiency and yield of rainfed and irrigated tomato. Int. J. Agric. Biol. 13, 469–476.

Aggarwal, K.P., Kumar, N.S., Pathak, H., 2010. Impacts of climate change on growth and yield of rice and wheat in the Upper Ganga Basin. Indian Agricultural Research Institute (IARI) (WWF-India, 172-B, Lodi Estate, New Delhi).

Akpalu, W., Hassan, R.M., Ringler, C., 2008. Climate variability and maize yield in South Africa: results from GME and MELE methods. Environ. Prod. Technol. 1–12.

Alvarez, R., Alvarez, C., 2001. Temperature regulation of soil carbon dioxide production in the humid pampa of Argentina: estimation of carbon fluxes under climate change. Biol. Fertil. Soils 34 (4), 282–285.

Arnold, J.G., Moriasi, D.N., Gassman, P.W., Abbaspour, K.C., White, M.J., Srinivasan, R., Jha, M.K., 2012. SWAT: model use, calibration, and validation. Trans. ASABE 55, 1491–1508.

Arunrat, N., 2017. Management Practices and Climate Change Influencing on Rice Yield and Soil Organic Carbon in Northeast Thailand. Division of Environment Resources, Graduate School of Agriculture, Hokkaido University (Doctoral Thesis).

Asseng, S., Foster, I.A.N., Turner, N.C., 2011. The impact of temperature variability on wheat yield. Glob. Chang. Biol. 17, 997–1012.

Babur, M., Babel, M., Shrestha, S., Kawasaki, A., Tripathi, N., 2016. Assessment of climate change impact on reservoir inflows using multi climate-models under RCPs—the case of Mangla dam in Pakistan. Water 8 (9), 389.

Balkovic, J., Schmid, E., Skalsky, R., Novakova, M., 2011. Modelling soil organic carbon changes on arable land under climate change - a case study analysis of the Kocin farm in Slovakia. Soil Water Res. 6 (1), 30–42.

Bangkok bank, 2003. The Chemical Fertilizer Industry. http://www.bangkokbank.com/download/The%20Chemical%20Fertilizer%20Industry.pdf (Verified Oct, 2016).

Bhattarai, M.D., Secchi, S., Schoof, J., 2017. Projecting corn and soybeans yields under climate change in a Corn Belt watershed. Agric. Syst. 152, 90–99.

Bocchiola, D., 2015. Impact of potential climate change on crop yield and water footprint of rice in the Po valley of Italy. Agric. Syst. 139, 223–237.

Brady, N.C., Weil, R.R., 1999. The Nature and Properties of Soils, 12th Ed. Prentice-Hall, Inc., Upper Saddle River, NJ (881p).

Brown, R.A., Rosenberg, N.J., Hays, C.J., Easterling, W.E., Mearns, L.O., 2000. Potential production and environmental effects of switchgrass and traditional crops under current and greenhouse-altered climate in the Central United States: a simulation study. Agric. Ecosyst. Environ. 78, 31–47.

Candradijaya, A., Kusmana, C., Syaukat, Y., Syaufina, L., Faqih, A., 2014. Climate change impact on Rice yield and adaptation response of local farmers in Sumedang District, west java, Indonesia. Int. J. Ecosyst. 4 (5), 212–223.

Carney, K.M., Hungate, B.A., Drake, B.G., Megonigal, J.P., 2007. Altered soil microbial community at elevated CO_2 leads to loss of soil carbon. Proc. Natl. Acad. Sci. U. S. A. 104, 4990–4995.

Causarano, H.J., Shaw, J.N., Franzluebbers, A.J., Reeves, D.W., Raper, R.L., Balkcom, K.S., Norfleet, M.L., Izaurralde, R.C., 2007. Simulating field-scale soil organic carbon dynamics using EPIC. Soil Sci. Soc. Am. J. 71, 1174–1185.

Causarano, H.J., Doraiswamy, P.C., McCarty, G.W., Hatfield, J.L., Milak, S., Stern, A.J., 2008. EPIC modeling of soil organic carbon sequestration in croplands of Iowa. J. Environ. Qual. 37, 1345–1353.

Causarano, H.J., Doraiswamy, P.C., Muratova, N., Pachikin, K., McCarty, G.W., Akhmedov, B., Williams, J.R., 2011. Improved modeling of soil organic carbon in a semiarid region of Central East Kazakhstan using EPIC. Agron. Sustain. Dev. 31, 275–286.

Caylor, K.K., Shugart, H.H., 2004. Simulated productivity of heterogeneous patches inSouthern African savanna landscapes using a canopy productivity model. Landsc. Ecol. 19, 401–415.

Chung, S.W., Gasman, P.W., Huggins, D.R., Randall, G.W., 2001. EPIC tile flow and nitrate loss predictions for three Minnesota cropping system. J. Environ. Qual. 30, 822–830.

Conant, R., Drijber, R.A., Haddix, M.L., Parton, W., Paul, E.A., Plante, A., Six, J., Steinweg, J.M., 2008. Sensitivity of organic matter decomposition to warming varies with its quality. Glob. Chang. Biol. 14, 868–877.

Curiel, J., Janssens, I.A., Carrara, A., Ceulemans, R., 2004. Annual Q10 of soil respiration

reflects plant phenological patterns as well as temperature sensitivity. Glob. Chang. Biol. 10, 161–169.
Dintwe, K., Okin, G.S., 2018. Soil organic carbon in savannas decreases with anthropogenic climate change. Geoderma 309, 7–16.
Dintwe, K., Okin, G.S., D'Odorico, P., Hrast, T., Mladenov, N., Handorean, A., Bhattachan, A., Caylor, K.K., 2014. Soil organic C and total N pools in the Kalahari: potentialimpacts of climate change on C sequestration in savannas. Plant Soil 396, 27–44.
Downing, T., 1992. Climate change and vulnerable places: global food security and country studies in Zimbabwe, Kenya, Senegal and Chile. Research Report No. 1. Oxford, Environmental Change Unit, University of Oxford.
Easterling, W.E., Weiss, A., Hays, C.J., Mearns, L.O., 1998. Spatial scales of climate information for simulating wheat and maize productivity: the case of the US Great Plains. Agric. For. Meteorol. 90, 51–63.
Erda, L., Yinlong, X., Hui, J., Wei, X., 2004. Possible adaptation decisions from investigating the impacts of future climate change on food and water supply in China. In: Paper Presented at the 2nd AIACC Regional Workshop for Asia and the Pacific, 2–5 November 2004, (Manila, Philippines).
Erda, L., Wei, X., Hui, J., Yinlong, X., Yue, L., Liping, B., Liyong, X., 2005. Climate Change impacts on crop yield and quality with CO_2 fertilization in China. Philos. Trans. R. Soc. B 360 (1463), 2149–2154 (29).
Furuya, J., Koyama, O., 2005. Impacts of climatic change on world agricultural product markets: estimation of macro yield functions. Jpn. Agric. Res. Q. 39 (2), 121–134.
Gaiser, T., Stahr, K., Billen, N., Mohammad, M.A., 2008. Modeling carbon sequestration under zero tillage at the regional scale: 1. The effect of soil erosion. Ecol. Model. 218, 110–120.
Gaiser, T., De Barros, I., Sereke, F., Lange, F.-M., 2010. Validation and reliability of the EPIC model to simulate maize production in small-holder farming systems in tropical sub-humid West Africa and semi-arid Brazil. Agric. Ecosyst. Environ. 135, 318–327.
Gifford, R., 1994. The global carbon cycle: a viewpoint on the missing sink. Aust. J. Plant Physiol. 21 (1), 1–15.
Goebel, M.O., Bachmann, J., Reichstein, M., Janssens, I.V., Guggenberger, J., 2011. Soil water repellency and its implications for organic matter decomposition—is there a link to extreme climatic events. Glob. Chang. Biol. 17, 2640–2656.
Gottschalk, P., Smith, J.U., Wattenbach, M., Bellarby, J., Stehfest, E., Arnell, N.W., Osborn, T.J., Jones, C., Smith, P., 2012. How will organic carbon stocks in mineral soils evolveunder future climate global projections using Roth C for a range of climate changescenarios. Biogeosciences 9 (8), 3151–3171.
Guerra, L.C., Hoogenboom, G., Boken, V.K., Hook, J.E., Thomas, D.L., Harrison, K.A., 2004. Evaluation of the EPIC model for simulating crop yield and irrigation demand. Trans. ASAE. 47, 2091–2100.
Heisler, J.L., Weltzin, J.F., 2006. Variability matters: towards a perspective on the influence of precipitation on terrestrial ecosystems. New Phytol. 172, 189–192.
Hobley, E.U., Wilson, B., 2016. The depth distribution of organic carbon in the soils of eastern Australia. Ecosphere. 7. (n/a-n/a).
Hogy, P., Fangmeier, A., 2008. Effects of elevated atmospheric CO_2 on grain quality of wheat. J. Cereal Sci. 48, 580–591.
IPCC, 2013. In Climate Change 2013: The Physical Science Basic Contribution of WorkingGroup 1 to the Fifth Assessment Report of the Intergovernmental Panel on Climate Change. Cambridge University Press, Cambridge, United Kingdom and New York, USA.
Izaurralde, R.C., Williams, J.R., McGill, W.B., Rosenberg, N.J., 2001. Simulating Soil Carbon Dynamics, Erosion, and Tillage with EPIC. In: Proc. 1st National Conference on Carbon Sequestration. Department of Energy – National Energy Technology Laboratory. Washington D.C, U.S., pp. 1–12.
Izaurralde, R.C., Rosenberg, N.J., Brown, R.A., Thomson, A.M., 2003. Integrated assessment of Hadley Centre (HadCM2) climate change projections on agricultural productivity and irrigation water supply in the conterminous United States-I. Regional agricultural production in 2030 and 2095. Agric. For. Meteorol. 117, 97–122.
Izaurralde, R.C., Williams, J.R., McGill, W.B., Rosenberg, N.J., Quiroga Jakas, M.C., 2006. Simulating soil C dynamics with EPIC: model description and testing against long-term data. Ecol. Model. 192, 362–384.
Jinger, D., Kaur, R., Kaur, N., Dass, A., 2017. Weed dynamics under changing climatic scenario: a review. Int. J. Curr. Microbiol. and Appl. Sci. 6, 2376–2388.
Kant, S., Seneweera, S., Rodin, J., Materne, M., Burch, D., Rothstein, S.J., Spangenberg, G., 2012. Improving yield potential in crops under elevated CO_2: integrating the photosynthetic and nitrogen utilization efficiencies. Front. Plant Sci. 3, 162.
Kelly, R.H., Parton, W.J., Crocker, G.J., Grace, P.R., Klír, J., Körschens, M., Poulton, P.R., Richter, D.D., 1997. Simulating trends in soil organic carbon in long-term experiments using the century model. Geoderma 81, 75–90.
Kimball, B.A., 1983. Carbon dioxide and agricultural yield: an assemblage and analysis of 430 prior observations1. Agron. J. 75, 779–788.
Kimball, B.A., Kobayashi, K., Bindi, M., 2002. Responses of agricultural crops to free-air CO_2 enrichment. In: Sparks, D.L. (Ed.), Advances in Agronomy. Academic Press, pp. 293–368.
Lal, R., 2003. Carbon sequestration in dryland ecosystems. Environ. Manag. 33, 528–544.
Lal, R., 2008. Carbon sequestration. Phil. Trans. R. Soc. B Biol. Sci. 363, 815–830.
Land Development Department (LDD), 1991. Distribution of Salt Affected Soil in the Northeast Region 1:100,000 Map. Ministry of Agriculture and Cooperatives, Thailand (Land Development Department).
Lesk, C., Rowhani, P., Ramankutty, N., 2016. Influence of extreme weather disasters onglobal crop production. Nature 529, 84–87.
Li, J.T., Zhang, B., 2007. Paddy soil stability and mechanical properties as affected by long-term application of chemical fertilizer and animal manure in subtropical China. Pedosphere 17 (5), 568–579.
Li, Z.P., Liu, M., Wu, X.C., Han, F.X., Zhang, T.L., 2010. Effects of long-term chemical fertilization and organic amendments on dynamics of soil organic C and total N in paddy soil derived from barren land in subtropical China. Soil Tillage Res. 106 (2), 268–274.
Li, X., Zhang, X., Zhang, Y., 2011. Modeling the effects of climate change and elevated CO_2 on soil organic carbon in an alpine steppe. J. Resour. and Ecol. 2 (2), 168–174.
Limjirakan, S., Limsakul, A., 2012. Observed trends in surface air temperatures and their extremes in Thailand from 1970 to 2009. J. Meteorol. Soc. Jpn. 90 (5), 647–662.
Limsakul, A., Limjirakan, S., Sriburi, T., 2010. Observed changes in daily rainfall extreme along Thailand' coastal zones. J. Environ. Res. 32 (1), 49–68.
Lin, E., Xiong, W., Ju, H., Xu, Y., Li, Y., Bai, L., Liyong, X., 2005. Climate change impacts on crop yield and quality with CO_2 fertilization in China. Philos. Trans. R. Soc. 360, 2149–2154.
Liu, J., 2009. A GIS-based tool for modelling large-scale crop-water relations. Environ. Model Softw. 24, 411–422.
Liu, M., He, B., Lü, A., Zhou, L., Wu, J., 2014. Parameters sensitivity analysis for a crop growth model applied to winter wheat in the Huanghuaihai plain in China. Geosci. Model Dev. Discuss. 7, 3867–3888.
Long, S.P., Ainsworth, E.A., Leakey, A.D.B., Morgan, P.B., 2005. Global food insecurity. Treatment of major food crops with elevated carbon dioxide or ozone under large-scale fully open-air conditions suggests recent models may have overestimated future yields. Phil. Trans. R. Soc. B Biol. Sci. 360, 2011–2020.
Mack, M.C., Schuur, E.A.G., Bret-Harte, M.S., Shaver, G.R., Chapin, F.S., 2004. Ecosystem carbon storage in arctic tundra reduced by long-term nutrient fertilization. Nature 431, 440–443.
McGrath, J.M., Lobell, D.B., 2013. Regional disparities in the CO_2 fertilization effect and implications for crop yields. Environ. Res. Lett. 8, 014054.
Meier, I.C., Leuschner, C., 2010. Variation of soil and biomass carbon pools in beech forests across a precipitation gradient. Global Change Biol. 16, 1035–1045.
Mott, K.A., 1988. Do stomata respond to CO_2 concentrations other than intercellular? Plant Physiol. 86, 200–203.
Nakano, H., Makino, A., Mae, T., 1997. The effect of elevated CO_2 partial pressure of CO_2 on the relationship between photosynthetic capacity and N content in rice leaves. Plant Physiol. 115, 191–198.
Nash, J.E., Sutcliffe, J.V., 1970. River flow forecasting through conceptual models: part I. A discussion of principles. J. Hydrol. 10 (3), 282–290.
Nelson, G.C., Valin, H., Sands, R.D., Havlík, P., Ahammad, H., Deryng, D., 2014. Climate change effects on agriculture: economic responses to biophysical shocks. Proc. Natl. Acad. Sci. 111 (9), 3274–3279.
Nguyen, N.V., 2006. Global Climate Changes and RExecutive Secretaryice Food Security. International Rice Commission, FAO, Rome, Italy (Executive Secretary).
Ni, J., 2001. Carbon storage in terrestrial ecosystems of China: estimates at different spatial resolutions and their responses to climate change. Clim. Chang. 49 (3), 339–358.
Nie, M., Pendall, E., Bell, C., Gasch, C.K., Raut, S., Tamang, S., Wallen-stein, M.D., 2013. Positive climate feedbacks of soil microbial communities in a semiarid grassland. Ecol. Lett. 16, 234–241.
Niu, X., Easterling, W., Hays, C.J., Jacobs, A., Mearns, L., 2009. Reliability and input-data induced uncertainty of the EPIC model to estimate climate change impact on sorghum yields in the U.S. Great Plains. Agric. Ecosyst. Environ. 129, 268–276.
OAE (Office of Agricultural Economics), 2014. Agricultural Statistics of Thailand; 2014; (in Thai Verified Feb, 2015) http://www.oae.go.th/download/download_journal/2558/yearbook57.pdf
Ojima, D.S., Dirks, B.O.M., Glenn, E.P., Owensby, C.E., Scurlock, J.O., 1993. Assessment of C budget for grasslands and drylands of the world. Water Air Soil Pollut. 70, 95–109.
Oteng-Darko, P., Kyei-Baffour, N., Ofori, E., 2012. Simulating rice yields under climate change scenarios using the CERES-Rice model. Afr. Crop. Sci. J. 20 (2), 401–408.
Ottman, M.J., Kimball, B.A., White, J.W., Wall, G.W., 2012. Wheat growth response to increased temperature from varied planting dates and supplemental infrared heating. Agron. J. 104, 7–16.
Owensby, C.E., Coyne, P.I., Ham, J.M., Auen, L.M., Knapp, A.K., 1993. Biomass production in a tallgrass prairie ecosystem exposed to ambient and elevated CO_2. Ecol. Appl. 3 (4), 644–653.
Parry, M., Rosenzweig, C., Iglesias, A., Liermore, M., Fischer, G., 2004. Effects of climate change on global food production under Sres emissions and socio-economic scenarios. Glob. Environ. Chang. 14 (1), 53–67.
Parton, W.J., Schimel, D.S., Cole, C.V., Ojima, D.S., 1987. Analysis of factors controlling soil organic matter levels in Great Plains grasslands. Soil Sci. Soc. Am. J. 51, 1173–1179.
Parton, W.J., Scurlock, J.M.O., Ojima, D.S., Gilmanov, T.G., Scholes, R.J., Schimel, D.S., Kirchner, T., Menaut, J.-C., Seastedt, T., Garcia, E., Moya Kamnalrut, A., Kinyamario, J.I., 1993. Observations and modelling of biomass and soil organic matter dynamics for the grassland biome worldwide. Global Biogeochem. Cycles 7, 785–809.
Parton, W.J., Ojima, D.S., Cole, C.V., Schimel, D.S., 1994. A general model for soil organic matter dynamics: Sensitivity to litter chemistry, texture and management. In: Quantitative Modeling of Soil Forming Processes. SSSA Spec. Public, Madison, WI, pp. 147–167 (No. 39 SSSA).
Parton, W., Scholes, R., Day, K., Carter, J., Kelly, R., 2010. In: Hill, M., Hanan, N. (Eds.), Century-Savanna Model for Tree–Grass Ecosystems. CRC Press, Ecosystem Function in Savannas, pp. 443–461.
Patterson, D.T., Flint, E.P., 1980. Potential effects of global atmospheric CO_2 enrichment on the growth and competitiveness of C_3 and C_4 weed and crop plants. Weed Sci. 28, 71–75.
Porter, J.R., Gawith, M., 1999. Temperatures and the growth and development of wheat: a review. Eur. J. Agron. 10, 23–36.
Ringius, L., 2002. Soil carbon sequestration and the CDM: opportunities and challenges for Africa. Climate Change 54, 471–495.

Rosenberg, N.J., 1981. The increasing CO_2 concentration in the atmosphere and its implication on agricultural productivity. Climate Change 3, 265–279.
Rosenzweig, C., Iglesis, A., 1994. Implications of Climate Change for International Agriculture: Crop Modeling Study. US Environmental Protection Agency, Climate Change Division, Washington DC.
Salvador Sanchis, M.P., Torri, D., Borselli, L., Poesen, J., 2008. Climate effects on soil erodibility. Earth Surf. Process. Landf. 33, 1082–1097.
Santhi, C., Arnold, J.G., Williams, J.R., Dugas, W.A., Srinivasan, R., Hauck, L.M., 2001. Validation of the SWAT model on a large river basin with point and nonpoint sources. J. Am. Water Res. Assoc. 37 (5), 1169–1188.
Schaeffer, S.M., Sharp, E., Schimel, J.P., Welker, J.M., 2013. Soil-plant N processes in a high Arctic ecosystem, NW Greenland are altered by longterm experimental warming and higher rainfall. Glob. Chang. Biol. 19, 3529–3539.
Sharpley, A.N., Wiliams, J.R., 1990. EPIC The Erosion Productivity Impact Calculator. 1. Model Documentation. U.S. Department of Agriculture (Technical Buletin No. 1768).
Shen, S.H., Yang, S.B., Zhao, Y.X., Xu, Y.L., Zhao, X.Y., Wang, Z.Y., Liu, J., Zhang, W.W., 2011. Simulating the rice yield change in the middle and lower reaches of the Yangtze River under SRES B2 scenario. Acta Ecol. Sin. 31, 40–48.
Shimono, H.O.M., Yamakawa, Y., Nakamura, H., Kobayashi, K., Hasegawa, T., 2009. Genotypic variation in rice yield enhancement by elevated CO2 relates to growth before heading and not to maturity group. J. Exp. Biol. 60, 523–532.
Smith, P., Smith, J.U., Powlson, D.S., McGill, W.B., Arah, J.R.M., Chertov, O.G., 1997. A comparison of the performance of nine soil organic matter models using datasets from seven long-term experiments. Geoderma 81, 153–225.
Smith, J., Smith, P., Wattenbach, M., Zaehle, S., Hiederer, R., Jones, R.J.A., Montanarella, L., Rounsevell, M., Reginster, I., Ewert, F., 2005. Projected changes in mineral soil carbon of European croplands and grasslands, 1990-2080. Glob. Chang. Biol. 11, 2141–2152.
Tack, J., Barkley, A., Nalley, L.L., 2015. Effect of warming temperatures on US wheat yields. Proc. Natl. Acad. Sci. U. S. A. 112, 6931–6936.
Tao, F.L., Yokozawa, M., Xu, Y.L., Hayashi, Y., Zhang, Z., 2006. Climate changes and trends in phenology and yields of field crops in China, 1981–2000. Agric. For. Meteorol. 138, 82–92.
Tao, F.L., Zhang, Z., Xiao, D.P., Zhang, S., Rotter, R.P., Shi, W.J., Liu, Y.J., Wang, M., Liu, F.S., Zhang, H., 2014. Responses of wheat growth and yield to climate change in different climate zones of China, 1981–2009. Agric. For. Meteorol. 189/190, 91–104.
Taylor, K.E., Stouffer, R.J., Meehl, G.A., 2012. An overview of CMIP5 and the experiment design. Bull. Am. Meteorol. Soc. 93, 485–498.
Thomas, A.D., Hoon, S.R., Dougill, A.J., 2011. Soil respiration at five sites along theKalahari transect: effects of temperature precipitation pulses and biological soil crust cover. Geoderma 167–168, 284–294.
Thomson, A.M., Brown, R.A., Rosenberg, N.J., Izaurralde, R.C., Benson, V., 2005. Climate change impacts for the conterminous USA an integrated assessment. Climate Change 69, 43–65.
Van Groenigen, K.J., Osenberg, C.W., Hungate, B.A., 2011. Increased soil emissions of potent greenhouse gases under increased atmospheric CO2. Nature 475 (7355), 214–216.
Van Groenigen, K.V., Craig, W., Osenberg, C.T., Yolima, C., Feike, A., Dijkstra, J.H., Ming, N., Elise, P., Richard, P.P., Bruce, A.H., 2017. Faster turnover of new soil carbon inputs under increased atmospheric CO2. Global Change Biol. 23, 4420–4429.
Van Vuuren, D., Edmonds, J., Kainuma, M., Riahi, K., Thomson, A., Hibbard, K., Hurtt, G., Kram, T., Krey, V., Lamarque, J.-F., Masui, T., Meinshausen, M., Nakicenovic, N., Smith, S., Rose, S., 2011. The representative concentration pathways an overview. Clim. Chang. 109, 5–31.
Wang, X.C., Li, J., 2010. Evaluation of crop yield and soil water estimates using the EPIC model for the loess plateau of China. Math. Comput. Model. 51, 1390–1397.
Wang, X., He, X., Williams, J.R., Izaurralde, R.C., Atwood, J.D., 2005. Sensitivity and uncertainty analyses of crop yields and soil organic carbon simulated with EPIC. Trans. ASAE 48 (3), 1041–1054.
Wang, X., Williams, J.R., Gassman, P.W., Baffaut, C., Izaurralde, R.C., Jeong, J., Kiniry, J.R., 2012. EPIC and APEX model use calibration and validation. Trans. ASABE 55, 1447–1462.
Williams, J.R., Jones, C.A., Dyke, P.T., 1984. A modeling approach to determining the relationship between erosion and soil productivity. Trans. ASAE 27, 129–144.
Williams, J.R., Jones, C.A., Kiniry, J.R., Spanel, D.A., 1989. The EPIC crop growth model. Trans. ASAE 32 (2), 497–511.
Williams, J.R., Wang, E., Meinardus, A., Harman, W.L., Siemers, M., Atwood, J.D., 2006. EPIC-Erosion Productivity Impact Calculator (Version 0509): User Guide. Blackland Research and Extension Center, Temple, TX.
Xiong, W., Holman, I., Conway, D., Lin, E.D., Li, Y., 2008. A crop model cross calibration for use in regional climate impacts studies. Ecol. Model. 213, 365–380.
Xiong, W., Balkovic, J., Velde, M., Zhang, X.S., Izaurralde, R.C., Skalsky, R., Lin, E.D., Mueller, N., Obersteiner, M., 2014. A calibration procedure to improve global rice yield simulations with EPIC. Ecol. Model. 273, 128–139.
Xu, L., Myneni, R.B., Chapin III, F.S., Callaghan, T.V., Pinzon, J.E., Tucker, C.J., Zhu, Z., Bi, J., Ciais, P., Tømmervik, H., Euskirchen, E.S., Forbes, B.C., Piao, S.L., Anderson, B.T., Ganguly, S., Nemani, R.R., Goetz, S.J., Beck, P.S., Bunn, A.G., Cao, C., Stroeve, J.C., 2013. Temperature and vegetation seasonality diminishment over northern lands. Nat. Clim. Chang. 3, 581–586.
Zhang, X.C., Nearing, M.A., Garbrecht, J.D., Steiner, J.L., 2004. Downscaling monthly forecasts to simulate impacts of climate change on soil erosion and wheat production. Soil Sci. Soc. Am. J. 68, 1376–1385.
Zhang, W.J., Wang, X.J., Xu, M.G., Huang, S.M., Liu, H., Peng, C., 2010. Soil organic carbon dynamics under long-term fertilizations in arable land of northern China. Biogeosciences 7, 409–425.
Zhang, Q., Singh, V.P., Sun, P., Chen, X., Zhang, Z., Li, J., 2011. Precipitation and stream flow changes in China: changing patterns causes and implications. J. Hydrol. 410, 204–216.
Zhao, X.N., Hu, K.L., Stahr, K., 2013. Simulation of SOC content and storage under different irrigation, fertilization and tillage conditions using EPIC model in the North China Plain. In: Soil & Tillage Research. 130. pp. 128–135.
Zhao, C., Piao, S., Huang, Y., Wang, X., Ciais, P., Huang, M., Zeng, Z., Peng, S., 2016. Field warming experiments shed light on the wheat yield response to temperature in China. Nat. Commun. 7, 13530.
Zhou, L.T., 2011. Impact of east Asian winter monsoon on rainfall over southeastern China and its dynamical process. Int. J. Climatol. 31 (5), 677–686.
Zhou, T., Shi, P., Hui, D., Luo, Y., 2009. Global pattern of temperature sensitivity of soil heterotrophic respiration (Q10) and its implications for carbon-climate feedback. J. Geophys. Res. 114, G02016.